

Pseudo-Labeling Curriculum for Unsupervised Domain Adaptation

Jaehoon Choi
whdns44@kaist.ac.kr

Minki Jeong
rhm033@kaist.ac.kr

Taekyung Kim
tkkim93@kaist.ac.kr

Changick Kim
changick@kaist.ac.kr

School of Electrical Engineering
Korea Advanced Institute of Science
and Technology (KAIST)
Daejeon, Korea

Abstract

To learn target discriminative representations, using pseudo-labels is a simple yet effective approach for unsupervised domain adaptation. However, the existence of false pseudo-labels, which may have a detrimental influence on learning target representations, remains a major challenge. To overcome this issue, we propose a pseudo-labeling curriculum based on a density-based clustering algorithm. Since samples with high density values are more likely to have correct pseudo-labels, we leverage these subsets to train our target network at the early stage, and utilize data subsets with low density values at the later stage. We can progressively improve the capability of our network to generate pseudo-labels, and thus these target samples with pseudo-labels are effective for training our model. Moreover, we present a clustering constraint to enhance the discriminative power of the learned target features. Our approach achieves state-of-the-art performance on three benchmarks: *Office-31*, *imageCLEF-DA*, and *Office-Home*.

1 Introduction

In computer vision, large-scale datasets have played an essential role in the success of deep neural networks. However, creating a large amount of labeled data is expensive and time-consuming. To overcome this problem, unsupervised domain adaptation approaches leverage the labeled data in a source domain to train a high-performance model on unlabeled data in a target domain. Such unsupervised domain adaptation methods suffer from the covariate shift between source and target data distributions due to different characteristics of both domains [5]. To tackle the covariate shift problem, many domain adaptation methods aim to jointly learn domain-invariant representations by minimizing domain divergence [4].

Recently, adversarial domain adaptation methods [4, 56] have received lots of attention. Similar to generative adversarial networks (GANs) [8], these methods employ two players, namely domain discriminator and feature extractor, to align feature distributions across domains in an adversarial manner. The core module for domain adaptation is domain discriminator, which is trained to discriminate the domain labels of features generated by the

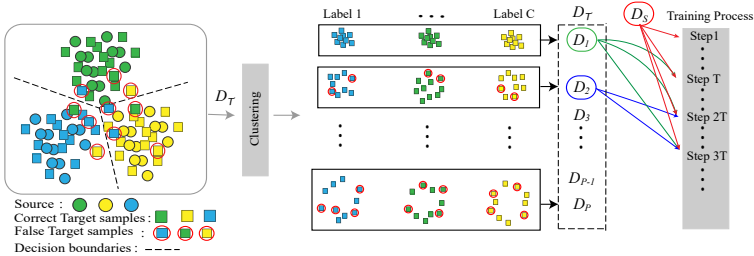


Figure 1: Learning process of the proposed method. D_S is a set of all source samples, and D_T is a set of all target samples. D_1, D_2, \dots , and D_p are data subsets obtained from D_T . C is the number of classes. By using a density-based clustering algorithm, we split our target dataset into a number of data subsets for each category and give these subsets following training process.

feature extractor. Conversely, the feature extractor is trained to provide transferable features that fool the domain discriminator by minimizing the divergence between features generated from the source and the target domain. Although their general efficacy shows impressive results in various tasks like segmentation [14, 35], detection [9, 13], and depth estimation [22], the adversarial domain adaptation methods suffer from a major problem. Since the domain discriminator only focuses on aligning global domain features, these methods often fail to consider the category information of target samples. Thus, category-level domain alignment enforced by adversarial domain adaptation methods does not guarantee the good target performance due to the lack of categorical target information [22]. To learn target categorical representation, recent studies [52, 58, 69] utilize pseudo-labels for target samples, thus encouraging a low-density separation between classes [15]. Although these methods rely on the assumption that the source-trained classifier assigns pseudo-labels to target samples with high confidence, it is difficult to satisfy this assumption especially when domain discrepancy is large. Training the network with false pseudo-labels may degrade the capability of distinguishing discriminant target samples by accumulating classification errors.

To alleviate this issue, we introduce a curriculum learning strategy for unsupervised domain adaptation. The curriculum learning [2] is motivated by the cognitive process of humans that gradually learn from easy to complex samples. Inspired by this concept, we propose a novel algorithm called pseudo-labeling curriculum for unsupervised domain adaptation (PCDA). For designing this pseudo-labelling curriculum, we apply a density-based clustering algorithm in [9] to divide target dataset into a number of data subsets relying on both pseudo-labels and features generated by our network. Then, we sequentially train target specific network from target samples whose pseudo-labels have a high chance of being correct to those which are highly likely to be misclassified. Our learning process is demonstrated in Fig. 1. In this process, we only use some target data subsets with correct pseudo-labels at the early training stage. As the training proceeds, our classifier can generate progressively reliable pseudo-labels for other target data subsets which are utilized at the later stage. Training with the pseudo-labeling curriculum boosts the robustness of the training target specific network with pseudo-labels by sequentially providing target data subsets. PCDA is effective to suppress the negative influence of false pseudo-labeled target samples. Furthermore, we suggest the constraints for clustering on the target data to reduce the intra-class variance of target representations and to enlarge the inter-class variance of target representations. This constraint reinforces the assumption of the density-based clustering that target samples with a high density value are more likely to have correct pseudo-labels. Our experimental results

suggest that PCDA achieves comparable or even better results compared with the state-of-the-art domain adaptation methods.

2 Related Works

Several types of adversarial learning methods for unsupervised domain adaptation have been shown to match distributions of the features generated from source and target examples ([10], [12], [8], [19], [36], [27]). However, they mainly focus on aligning domain-level feature distributions without considering category-level alignment. Xie *et al.* [38] match the labeled source centroid and the pseudo-labeled target centroid to learn semantic representations for target samples. This moving average centroid alignment guides the feature extractor to consider category-level information for target samples. Pei *et al.* [23] exploit multiple domain discriminators to enable fine-grained distribution alignment.

Some studies [4, 26, 30, 32, 39] use pseudo-labeled target samples to learn target discriminative representations. Sener *et al.* [30] adopt clustering techniques and pseudo-labels to learn discriminative features. In [32] and [8], they apply a Mean Teacher framework [34] to domain adaptation with the consistency regularization. Saito *et al.* [26] employ the asymmetric tri-training (ATT), which leverages target samples labeled by the source-trained classifier to learn target discriminative features. Zhang *et al.* [39] iteratively select pseudo-labeled target samples based on their proposed criterion and retrain the model with a training set including pseudo-labeled samples. However, these methods based on pseudo-labeled target samples have a critical bottleneck that false pseudo-labels can impede learning target discriminative features and further their categorical error is easily accumulated, which hurt the performance.

Curriculum learning proposed by [1] is a learning paradigm based on ranking the training samples from easiest to the most difficult to classify. The curriculum based on ranking is used to guide the order of training procedure. Previous studies ([9, 12, 14, 16]) have demonstrated that curriculum learning is useful in handling problems with noisy labels. Guo *et al.* [9] propose a learning curriculum to handle massive, noisy sets of labels. They measure data complexity using cluster density and split all training samples into a number of subsets ordered by data complexity. By utilizing these subsets, they design a curriculum to train the network. We recast their strategy to design curriculum into our training algorithm.

3 Method

In this section, we explain details of the proposed algorithm. Our proposed network structure is demonstrated in Fig. 2. We let G_f denote the shared feature extractor for source and target data. C_s and C_t are classifiers which distinguish features generated from G_f . Here, θ_f , θ_s , and θ_t denote the model parameters of the respective G_f , C_s , and C_t . C_s learns from the source samples and C_t learns from pseudo-labeled target samples. G_d is the domain discriminator which aims to label all source samples as 1 and all target samples as 0. GRL stands for Gradient Reversal Layer, which inversely back-propagate gradients by changing the sign of the gradient [1]. The shared feature extractor G_f is trained from all gradients back-propagated by C_s , C_t , and G_d . Our goal is training C_t to be able to learn discriminative representations for the target domain. We have access to N_s labeled image samples from the source domain $D_S = \{(x_i^s, y_i^s)\}_{i=1}^{N_s}$ and N_t unlabeled image samples from the target domain

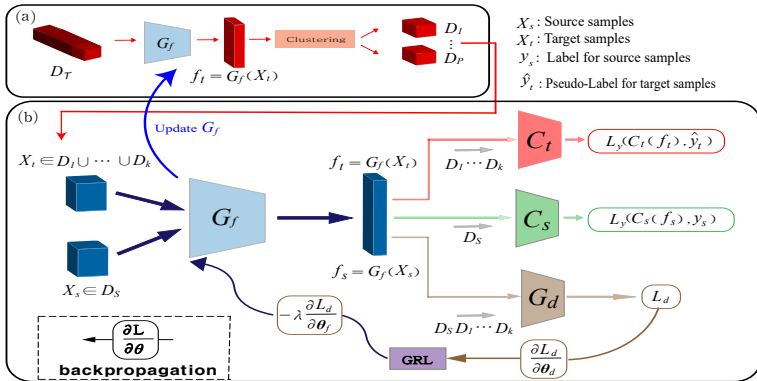


Figure 2: Pipeline of the proposed method: (a) The curriculum design from density-based clustering, (b) The structure of training our model. In (a), we use all target samples and pseudo-labels from C_s or C_t to generate data subsets, which form our curriculum for training our model. In (b), we train G_f , C_s , C_t and G_d with all source samples and selected data subsets of target samples following curriculum.

$D_{\mathcal{T}} = \{x_i^t\}_{i=1}^{N_t}$. \hat{y}_i^t denotes a pseudo-label for the target sample. We assume that D_S and $D_{\mathcal{T}}$ completely share the C classes.

3.1 Domain Adversarial Learning Scheme

Before obtaining pseudo-labeled target samples, we do not train the target specific classifier C_t . We only train G_f , C_s , and G_d by using supervised classification loss and domain adversarial loss following the idea of domain adversarial neural networks (DANN) [9]. The overall loss function in this stage is the following:

$$J_1(\theta_f, \theta_d, \theta_s) = \frac{1}{N_s} \sum_{i=1}^{N_s} L_y(C_s(f_i^s), y_i^s) - \frac{\lambda}{N_s} \sum_{i=1}^{N_s} L_d(G_d(f_i^s), d_i) - \frac{\lambda}{N_t} \sum_{i=1}^{N_t} L_d(G_d(f_i^t), d_i), \quad (1)$$

where L_y is the cross-entropy loss and L_d is the binary cross-entropy loss. f_i^s and f_i^t generated by G_f are the feature representations of source and target samples, i.e., $f_i^s = G_f(x_i^s)$ and $f_i^t = G_f(x_i^t)$. $d_i \in \{0, 1\}$ is the domain label and λ is a trade-off parameter. The overall objective is written as follows

$$\min_{\theta_f, \theta_s} \max_{\theta_d} J_1(\theta_f, \theta_d, \theta_s). \quad (2)$$

In the early stage of training, since C_s is highly likely to generate false pseudo-labeled target examples, we do not train C_t at all. After a few epochs, we start to train C_t with pseudo-labeled target examples.

3.2 Density-Based Clustering for Pseudo-Labeling Curriculum

We modify the curriculum learning method from [9] to enable domain adaptation. To design the curriculum, we should address two questions: how to rank the training samples, and how to construct the training schedule. We adopt the ranking method using their clustering density in order to split the target samples. C_s generates pseudo-labels \hat{y}_i^t for target samples and then it separates all features f_i^t into each category. Then, we conduct the following

process for each category. We first determine a matrix $\mathbf{E} \in \mathbb{R}^{n \times n}$, where n is the number of target samples in a certain category. The matrix \mathbf{E} is composed of elements $\mathbf{E}_{ij} = \|f_i^t - f_j^t\|^2$ indicating the Euclidean distance between f_i^t and f_j^t . A local density of each sample in a current category is defined as

$$\rho_i = \sum_j I(\mathbf{E}_{ij} - e_c), \quad I(x) = \begin{cases} 1 & x < 0 \\ 0 & \text{otherwise} \end{cases}. \quad (3)$$

We determine e_c by sorting all \mathbf{E}_{ij} elements in ascending order and select a number ranked at $k\%$ from the smallest value. We empirically set $k = 40$ in all experiments because the result of clustering is consistent when the value of k is between 40 and 70. The implication of ρ_i is the number of target samples whose distances are smaller than e_c .

Target samples with correct pseudo-labels often share similar visual characteristics, and thus features generated from these samples tend to form a cluster for each category. By contrast, target samples with a high chance of being false pseudo-labels often have a visual difference, leading to a sparse distribution which results in a small value of local density. Therefore, we select a sample with the highest local density value as a cluster center for each category. Since target samples close to the cluster center are more likely to have a correct pseudo-label, we divide target samples into a number of clusters according to their corresponding distances from the cluster center. For each category, we respectively apply the k-means algorithm to the set of distances between the target sample and cluster center for generating P clusters. Now, we acquire P clusters in each category, and each cluster can be thought of as a data subset, see Fig. 1. In all our experiments, we empirically set the number of clusters (P), *i.e.*, P to 3. Hence, each category contains three subsets, and we combine the overall categories. We can obtain three data subsets D_e , D_m , and D_h , which involve easy, moderate, and hard samples, respectively. The easy samples consist of target samples with a high density value, while the hard samples comprise target samples with a low density value.

In other words, it is challenging for the classifier C_s learned from the source samples to assign correct pseudo-labels for target samples due to the domain gap. In particular, the target samples far from corresponding cluster centers, or distributed near the boundary of the clusters are more likely to have false pseudo-labels. To minimize such an adverse effect, we firstly opt to use the data subset with low intra-class variance and high inter-class variance, such as the easy samples, at the early stage of training. By employing a subset with a high density value, the classifier C_t can learn target discriminative representations from correct pseudo-labeled target samples.

3.3 Training with Pseudo-Labeling Curriculum

Our training procedure is proceeded with four stages in conjunction with the ordered sequence of training subsets from easy to hard samples. At the first stage, we train G_f , C_s , and G_d with D_S and D_T , while C_t is not trained at all. It is described specifically in Section 3.1. Here G_f , C_s and G_d are optimized by Eq. (2). At the second stage, pseudo-labels for the easy samples $D_e = \{(x_i^t, \hat{y}_i^t)\}_{i=1}^{N_e}$ generated by C_s are highly reliable for training target classifier C_t . According to the terminology in Section 3.1, the loss function of the second stage can be

written as follows,

$$\begin{aligned}
 J_2(\theta_f, \theta_d, \theta_s, \theta_t) &= \frac{1}{N_s} \sum_{i=1}^{N_s} L_y(C_s(f_i^s), y_i^s) + \frac{1}{N_e} \sum_{i=1}^{N_e} L_y(C_t(f_i^t), \hat{y}_i^t) \\
 &\quad - \frac{\lambda}{N_s} \sum_{i=1}^{N_s} L_d(G_d(f_i), d_i) - \frac{\lambda}{N_e} \sum_{i=1}^{N_e} \beta L_d(G_d(f_i), d_i),
 \end{aligned} \tag{4}$$

where β is a hyperparameter that re-weights the contributions of the data subset which is newly added to the training process at the current stage. Compared to the early training samples which are already aligned between the source and target domains, the source and target features generated from newly added samples are poorly aligned. Then, the newly added samples may impede fine-tuning the feature extractor and learning the target classifier. A higher β value encourages the G_f to learn domain invariant features for the newly added samples. Thus, we enable effective domain adaptation based on the curriculum learning by focusing on the contribution of newly added samples. Third, we generate pseudo-labels for the easy samples D_e and the moderate samples D_m by using C_t and also train C_t with D_e and D_m . We use the same form of loss function in Eq. (4) with adding D_m . Lastly, the model is further trained by adding the hard samples D_h according to the learning strategy of the previous stage. Details are included in the supplementary material. We optimize the following minimax objective:

$$\min_{\theta_f, \theta_s, \theta_t} \max_{\theta_d} J_2(\theta_f, \theta_d, \theta_s, \theta_t). \tag{5}$$

3.4 Clustering Constraint

A clustering constraint is motivated by the need to boost the effectiveness of the density-based clustering algorithm in order to reduce the number of false pseudo-labeled target samples. For this purpose, the features from target samples with the same category should be as close as possible, while the features from target samples with different categories should be far from each other. We apply the concept of contrastive loss [5], which takes pairs of examples as input and trains a model to predict whether pairs of inputs are from the same category or not. Unlike [5, 29] which utilize all pairs of images as ground-truth labels, our method is based on the pseudo-labels in order to create pairs of inputs. We propose to formulate the Euclidean-based clustering loss (ECL) as follows,

$$J_{ECL}(C_t) = \sum_{\forall (i,j) \in \mathcal{T}} L_{ECL}(h_i, h_j), \quad L_{ECL}(h_i, h_j) = \begin{cases} \|h_i^t - h_j^t\|^2 & I_{ij} = 1 \\ \max(0, m - \|h_i^t - h_j^t\|)^2 & I_{ij} = 0 \end{cases}, \tag{6}$$

where h_i^t denotes the output of the target classifier C_t before the softmax layer with respect to the i -th training sample in the mini-batch. $\|\cdot\|^2$ is the squared Euclidean distance and $m > 0$ is a margin. $I_{ij} = 1$ means that h_i and h_j belong to the same category, while $I_{ij} = 0$ indicates that h_i and h_j are from the different categories. i and j denote the indices of target samples inside the mini-batch. The ECL loss encourages target features from the same category to be closer and enforce the distance between those from the different categories no more than m . This loss can be combined with J_2 in Eq. (4) to optimize G_f and C_t .

4 Experiments

4.1 Setups

Office-31 [25], the most popular benchmark dataset for visual domain adaptation, contains 4652 images and 31 categories from three distinct domains: *Amazon* (**A**), *Webcam* (**W**), and *DSLR* (**D**). We comprise all domain combinations and build 6 transfer tasks: **A**→**W**, **D**→**W**, **W**→**D**, **A**→**D**, **D**→**A**, and **W**→**A**.

ImageCLEF-DA¹, a benchmark dataset for Image-CLEF 2014 domain adaptation challenge, consists of three domains including *Caltech-256* (**C**), *ImageNet ILSVRC 2012* (**I**) and *Pascal VOC 2012* (**P**). Each domain contains 600 images and 50 images for each category. We evaluate our method on all possible domain adaptation tasks: **I**→**P**, **P**→**I**, **I**→**C**, **C**→**I**, **C**→**P**, and **P**→**C**. Different from Office-31, all images have equal size and the number of images in each category is well-balanced.

Office-Home [67], a more challenging dataset for domain adaptation evaluation, contains around 15,500 images with 65 categories consisting of four significantly different domains: Artistic images (**Ar**), Clipart images (**Cl**), Product images (**Pr**) and Real-World images (**Rw**). We can build possible twelve transfer tasks and evaluate our method on all possible tasks.

Implementation Details. The base network for both the baseline and our method is the ResNet-50 [10]. For domain discriminator, we chose to use the architecture consisting of three fully connected layers with dropout [53] and sigmoid layers. We fine-tuned all feature layers G_f pre-trained on the ImageNet dataset [24], following the standard settings for unsupervised domain adaptation [2, 19, 20]. The classifier layers C_s , C_t and the domain discriminator layers G_d are trained from the scratch via back-propagation. We set the learning rate of the feature extractor ten times smaller than other layers. According to the learning rate strategy employed in DANN [2], we utilized mini-batch stochastic gradient descent (SGD) with momentum of 0.9 and the learning rate adjusted by $\eta = \frac{\eta_0}{(1+\alpha p)^\gamma}$, where p is linearly increasing from 0 to 1, $\alpha = 10$, and $\gamma = 0.75$. The total batch size was set to 64, and we selected training samples for each stage in the mini-batch (D_e , D_m , D_h) as follows: (64, 0, 0), (32, 32, 0), and (32, 16, 16) for the stage 1 to 3 in all our experiments. Additionally, we set β to 2 or 3 in Eq. (4) and margin m to 2 in Eq. (6).

4.2 Evaluation Results

We complied with standard evaluation protocols for unsupervised domain adaptation [2] and used all source samples with labels and all target samples without labels. For all tasks, we performed three experiments and report the averaged results. We compare our methods with the basic ResNet50 [10], DAN [17], RTN [18], DANN [2], ADDA [66], JAN [19], GTA [28], CAN [69], and CDAN [20]. All these methods are based on ResNet50, and results of baselines are directly reported from original papers.

We report the classification accuracies of the networks in Table 1, Table 2, and Table 3. Our proposed PCDA is comparable with the state-of-the-art methods in that it achieves the best average accuracy on the three unsupervised domain adaptation benchmarks.

¹<https://www.imageclef.org/2014/adaptation>

Method	A→W	D→W	W→D	A→D	D→A	W→A	Avg
ResNet-50 [12]	68.4±0.2	96.7±0.1	99.3±0.1	68.9±0.2	62.5±0.3	60.7±0.3	76.1
DAN [12]	80.5±0.4	97.1±0.2	99.6±0.1	78.6±0.2	63.6±0.3	62.3±0.2	80.4
RTN [12]	84.5±0.2	96.8±0.1	99.4±0.1	77.5±0.3	66.2±0.2	64.8±0.3	81.6
DANN [12]	82.0±0.4	96.9±0.2	99.1±0.1	79.7±0.4	68.2±0.4	67.4±0.5	82.2
ADDA [12]	86.2±0.5	96.2±0.3	98.4±0.3	77.8±0.3	69.5±0.4	68.9±0.5	82.9
JAN [12]	85.4±0.3	97.4±0.2	99.8±0.2	84.7±0.3	68.6±0.3	70.0±0.4	84.3
GTA [12]	89.5±0.5	97.9±0.3	99.8±0.4	87.7±0.5	72.8±0.3	71.4±0.4	86.5
CAN [12]	92.5	98.8	100.0	90.1	72.1	69.9	87.2
CDAN [12]	93.1±0.1	98.6±0.1	100.0±0.0	92.9±0.2	71.0±0.3	69.3±0.3	87.5
PCDA (ours, wo ECL)	90.9±0.4	98.1±0.1	100.0±0.0	91.0±0.2	73.3±0.2	71.5±0.3	87.5
PCDA (ours)	92.5±0.3	98.7±0.2	100.0±0.0	93.0±0.2	73.5±0.3	72.5±0.3	88.3

Table 1: Accuracy(%) on *Office-31*.

Method	I→P	P→I	I→C	C→I	C→P	P→C	Avg
ResNet-50 [12]	74.8±0.3	83.9±0.1	91.5±0.3	78.0±0.2	65.5±0.3	91.2±0.3	80.7
DAN [12]	74.5±0.4	82.2±0.2	92.8±0.2	86.3±0.4	69.2±0.4	89.8±0.4	82.5
DANN [12]	75.0±0.6	86.0±0.3	96.2±0.4	87.0±0.5	74.3±0.5	91.5±0.6	85.0
JAN [12]	76.8±0.4	88.0±0.2	94.7±0.2	89.5±0.3	74.2±0.3	91.7±0.3	85.8
CAN [12]	79.5	89.7	94.7	89.9	78.5	92.0	87.4
CDAN [12]	78.3±0.3	91.2±0.2	96.7±0.3	91.2±0.3	77.2±0.2	93.7±0.3	88.1
PCDA (ours, wo ECL)	78.2±0.2	91.0±0.3	96.5±0.5	90.0±0.3	70.8±0.3	96.0±0.3	87.1
PCDA (ours)	80.2±0.2	92.5±0.3	96.7±0.3	90.3±0.1	75.2±0.3	97.0±0.1	88.7

Table 2: Accuracy(%) on *imageCLEF-DA*.

Method	Ar→Cl	Ar→Pr	Ar→Rw	Cl→Ar	Cl→Pr	Cl→Rw	Pr→Ar	Pr→Cl	Pr→Rw	Rw→Ar	Rw→Cl	Rw→Pr	Avg
ResNet-50 [12]	34.9	50.0	58.0	37.4	41.9	46.2	38.5	31.2	60.4	53.9	41.2	59.9	46.1
DAN [12]	43.6	57.0	67.9	45.8	56.5	60.4	44.0	43.6	67.7	63.1	51.5	74.3	56.3
DANN [12]	45.6	59.3	70.1	47.0	58.5	60.9	46.1	43.7	68.5	63.2	51.8	76.8	57.6
JAN [12]	45.9	61.2	68.9	50.4	59.7	61.0	45.8	43.4	70.3	63.9	52.4	76.8	58.3
CDAN [12]	50.6	65.9	73.4	55.7	62.7	64.2	51.8	49.1	74.5	68.2	56.9	80.7	62.8
PCDA (ours, wo ECL)	50.7	72.2	78.3	57.2	68.0	71.0	54.6	52.4	78.3	67.2	54.0	80.8	65.4
PCDA (ours)	50.8	73.7	78.5	58.6	70.4	71.2	53.9	53.5	79.0	65.6	53.6	80.2	65.8

Table 3: Accuracy(%) on *Office-Home*.

4.3 Analysis

Ablation Study. We perform an ablation study to check the efficacy of each component in our work. First of all, the above Tables 1, 2, and 3 show the results of PCDA (wo ECL) and PCDA. PCDA (wo ECL) denotes our training method without clustering constraint. The performance gap between PCDA and PCDA (wo ECL) in *Office31* and *imageCLEF-DA* demonstrate the effectiveness of the clustering constraint. However, regarding *Office-Home* experiment, PCDA with clustering constraint fails to enhance the classification performance in some tasks such as $Rw \rightarrow Cl$ and $Rw \rightarrow Ar$. This is presumably because the training method does not have sufficient mini-batch size to guarantee that similar pairs are somewhat sampled.

Hyperparameter Study. Our approach sets the hyperparameter β to learn domain-invariant features from newly added target samples. If β is one, our loss function for adversarial adaptation learning becomes equivalent to DANN’s loss function in Eq. (1). We used the *Office-31* dataset to validate the effectiveness of β in Table 4. When β is one, the performance of our training process degrades. In contrast, when we set β between 2 or 3, our method achieves better performance. This results prove our assumption that the weight β helps the network to extract domain invariant features for the newly added target samples.

The number of clusters P is important hyperparameter for our pseudo-labeling curriculum. When P is set to 4, We observe that most tasks in *Office-Home* shows performance improvement, while some tasks in *Office-31* present the performance degradation shown in Table 5. This is because large P is effective to improve models that tend to generate relatively many incorrect pseudo-labels for target samples. On the contrary, large P may not be helpful to enhance the capability of models which already show good performance on target data. We set P to 3 because the pseudo-labeling curriculum becomes simple to implement and achieves the best performance on all benchmarks.

Feature Visualization. To have an intuitive understanding of PCDA for domain adaptation, we visualize the target representations of the easy, moderate, and hard samples from the feature extractor G_f using t-SNE embedding [24] on the difficult $D \rightarrow A$ task. In Fig. 3(a), we can observe that the features of the easy samples in each category are tightly clustered and distinguishable from samples in the different categories. In contrast, those of the hard samples in each category are dispersed in Fig. 3(c). Since PCDA is developed from DANN, it is necessary to confirm whether the proposed model generates target discriminative features compared to DANN. We visualize the both source and target features of DANN and

	A→W	A→D	D→A	W→A
$\beta=1$	87.8	89.4	70.8	71.0
$\beta=2$	90.3	89.0	73.3	71.5
$\beta=3$	90.9	91.0	70.9	71.1

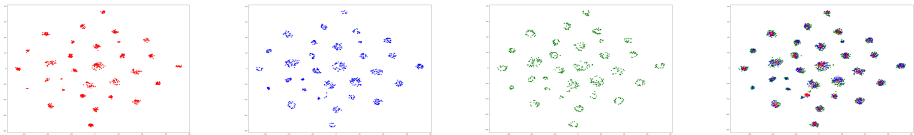
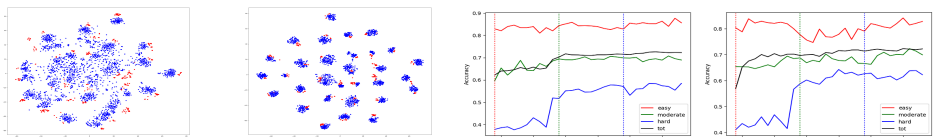
Table 4: The effectiveness of β .

	D→A	Ar→Pr
$P=2$	70.5	47.6
$P=3$	73.5	50.8
$P=4$	72.8	51.3

Table 5: The effectiveness of P .

	D→A	W→A	I→P	Cl→Rw
Model-1	70.4	70.3	76.2	70.6
Model-2	71.8	71.4	77.3	71.0
Model-3	73.3	72.5	80.2	71.2

Table 6: Test accuracy of three different models.

(a) Easy samples D_e (b) Moderate samples D_m (c) Hard samples D_h (d) All target samples D_T Figure 3: T-SNE visualization of features from easy, moderate, and hard samples by using our PCDA method on the $D \rightarrow A$ task.(a) DANN ($D \rightarrow A$) (b) PCDA ($D \rightarrow A$) (c) Test accuracy ($W \rightarrow A$) (d) Test accuracy ($D \rightarrow A$)Figure 4: On $D \rightarrow A$ task, (a) and (b) are T-SNE visualization of features. Red points are source samples and blue are target samples. (c) and (d) shows the comparison of test accuracy and pseudo-labeling accuracy. Red line, blue and green are pseudo-labeling accuracy of easy, moderate and hard target samples at every epoch. Black line is test accuracy of PCDA over the training epochs. The red vertical dotted line indicates the training epoch when the target data subset D_e is added for training our model. The green and blue vertical dotted lines are training epochs for adding D_m and D_h .

PCDA in Fig. 4(a) and Fig. 4(b). Compared with the features obtained by DANN (Fig. 4(a)), Fig. 4(b) indicates that PCDA learns more category-level discriminative features. The result corroborates the efficacy of our approach.

Effectiveness of Curriculum. To verify the effectiveness of pseudo-labeling curriculum, we evaluate three models for the comparison. We further investigated **Model-1** trained by only using the easy data subset D_e , **Model-2** trained by using D_e and the moderate data subset D_m with a 2-subset curriculum, and **Model-3** trained by using D_e , D_m , and D_h with a 3-subset curriculum. **Model-3** is equivalent to our proposed PCDA. In Table 6, **Model-3** outperforms other methods through most tasks. Although D_h is more likely to have false pseudo-labels, utilizing D_h is helpful for improving the test accuracies in most cases. It implies that the pseudo-labeling curriculum suppresses the adverse effects of the target samples with false pseudo-labels in most tasks. This table proves that our proposed method benefits the performance. However, regarding some challenging tasks in the *Office-Home* dataset such as $Rw \rightarrow Cl$ or $Pr \rightarrow Ar$, the usage of D_h slightly degrades the performance due to the excessive number of false-labeled target samples. Thus, if the target specific network C_t still provides too many false pseudo-labels for D_h , the effect of the pseudo-labeling curriculum degrades.

We report the test accuracy and pseudo-labeling accuracy in Fig. 4(c) and Fig. 4(d). The pseudo-labeling accuracy indicates whether pseudo-labels are assigned correctly. The test accuracy of our method is increasing when we give new additional target samples with

pseudo-labels such as D_m or D_h . These accord with our previous results in Table 6 in that supplementing target samples with generated pseudo-labels is effectual to boost the performance. We observe that the reliability of the generated pseudo-labels is improved iteratively as training proceeds. This proves that our training scheme with pseudo-labeling curriculum progressively improves the capability of our network to generate pseudo-labels and leads to better predictions. Moreover, the pseudo-labeling accuracies of easy samples are higher than those of both the moderate and hard samples in Fig. 4(c) and Fig. 4(d). Also, the pseudo-labeling accuracies of the moderate samples are higher than those of hard samples. These experimental results provide support for our main assumption that target samples with high density values are highly likely to have correct pseudo-labels. We confirm that this assumption is valid for all our experiments including Fig. 4(c) and Fig. 4(d).

5 Conclusion

We have proposed a novel learning scheme for unsupervised domain adaptation with the pseudo-labeling curriculum. Different from the existing works that exploit pseudo-labeled target samples, our method is robust to the adverse effect of false pseudo-labeled target samples due to the pseudo-labeling curriculum. The proposed method enables our model to generate reliable pseudo-labels progressively, and then the target specific network is able to learn target discriminative features. Furthermore, we introduce the clustering constraint on creating target features to improve the performance. Our approach surpasses the state-of-the-art classification results on three benchmarks. We also provide extensive analysis to validate the effectiveness of our method by utilizing visualization results and various ablation studies.

References

- [1] Shai Ben-David, John Blitzer, Koby Crammer, Alex Kulesza, Fernando Pereira, and Jennifer Wortman Vaughan. A theory of learning from different domains. *Machine learning*, 79(1-2):151–175, 2010.
- [2] Yoshua Bengio, Jérôme Louradour, Ronan Collobert, and Jason Weston. Curriculum learning. In *Proceedings of the 26th annual international conference on machine learning*, pages 41–48. ACM, 2009.
- [3] Konstantinos Bousmalis, George Trigeorgis, Nathan Silberman, Dilip Krishnan, and Dumitru Erhan. Domain separation networks. In *Advances in Neural Information Processing Systems*, pages 343–351, 2016.
- [4] Yuhua Chen, Wen Li, Christos Sakaridis, Dengxin Dai, and Luc Van Gool. Domain adaptive faster r-cnn for object detection in the wild. In *Proceedings of the IEEE conference on computer vision and pattern recognition*, pages 3339–3348, 2018.
- [5] Sumit Chopra, Raia Hadsell, and Yann LeCun. Learning a similarity metric discriminatively, with application to face verification. In *Computer Vision and Pattern Recognition, 2005. CVPR 2005. IEEE Computer Society Conference on*, volume 1, pages 539–546. IEEE, 2005.

- [6] Geoff French, Michal Mackiewicz, and Mark Fisher. Self-ensembling for visual domain adaptation. In *International Conference on Learning Representations*, 2018. URL <https://openreview.net/forum?id=rkpoTaxA->.
- [7] Yaroslav Ganin and Victor Lempitsky. Unsupervised domain adaptation by backpropagation. In *International Conference on Machine Learning*, pages 1180–1189, 2015.
- [8] Ian Goodfellow, Jean Pouget-Abadie, Mehdi Mirza, Bing Xu, David Warde-Farley, Sherjil Ozair, Aaron Courville, and Yoshua Bengio. Generative adversarial nets. In *Advances in neural information processing systems*, pages 2672–2680, 2014.
- [9] Sheng Guo, Weilin Huang, Haozhi Zhang, Chenfan Zhuang, Dengke Dong, Matthew R. Scott, and Dinglong Huang. Curriculumnet: Weakly supervised learning from large-scale web images. In *The European Conference on Computer Vision (ECCV)*, September 2018.
- [10] Kaiming He, Xiangyu Zhang, Shaoqing Ren, and Jian Sun. Deep residual learning for image recognition. In *Proceedings of the IEEE conference on computer vision and pattern recognition*, pages 770–778, 2016.
- [11] Judy Hoffman, Dequan Wang, Fisher Yu, and Trevor Darrell. Fcns in the wild: Pixel-level adversarial and constraint-based adaptation. *arXiv preprint arXiv:1612.02649*, 2016.
- [12] Lu Jiang, Zhengyuan Zhou, Thomas Leung, Li-Jia Li, and Li Fei-Fei. Mentornet: Learning data-driven curriculum for very deep neural networks on corrupted labels. In *International Conference on Machine Learning*, pages 2309–2318, 2018.
- [13] Taekyung Kim, Minki Jeong, Seunghyeon Kim, Seokeon Choi, and Changick Kim. Diversify and match: A domain adaptive representation learning paradigm for object detection. In *The IEEE Conference on Computer Vision and Pattern Recognition (CVPR)*, June 2019.
- [14] M Pawan Kumar, Benjamin Packer, and Daphne Koller. Self-paced learning for latent variable models. In *Advances in Neural Information Processing Systems*, pages 1189–1197, 2010.
- [15] Dong-Hyun Lee. Pseudo-label: The simple and efficient semi-supervised learning method for deep neural networks. In *Workshop on Challenges in Representation Learning, ICML*, volume 3, page 2, 2013.
- [16] Liang Lin, Keze Wang, Deyu Meng, Wangmeng Zuo, and Lei Zhang. Active self-paced learning for cost-effective and progressive face identification. *IEEE transactions on pattern analysis and machine intelligence*, 40(1):7–19, 2018.
- [17] Mingsheng Long, Yue Cao, Jianmin Wang, and Michael Jordan. Learning transferable features with deep adaptation networks. In *Proceedings of the 32nd International Conference on Machine Learning*, pages 97–105, 2015.
- [18] Mingsheng Long, Han Zhu, Jianmin Wang, and Michael I Jordan. Unsupervised domain adaptation with residual transfer networks. In *Advances in Neural Information Processing Systems*, pages 136–144, 2016.

- [19] Mingsheng Long, Han Zhu, Jianmin Wang, and Michael I. Jordan. Deep transfer learning with joint adaptation networks. In *Proceedings of the 34th International Conference on Machine Learning*, pages 2208–2217, 2017.
- [20] Mingsheng Long, ZHANGJIE CAO, Jianmin Wang, and Michael I Jordan. Conditional adversarial domain adaptation. In S. Bengio, H. Wallach, H. Larochelle, K. Grauman, N. Cesa-Bianchi, and R. Garnett, editors, *Advances in Neural Information Processing Systems 31*, pages 1647–1657. Curran Associates, Inc., 2018.
- [21] Laurens van der Maaten and Geoffrey Hinton. Visualizing data using t-sne. *Journal of machine learning research*, 9(Nov):2579–2605, 2008.
- [22] Jogendra Nath Kundu, Phani Krishna Uppala, Anuj Pahuja, and R Venkatesh Babu. Adadepth: Unsupervised content congruent adaptation for depth estimation. In *Proceedings of the IEEE Conference on Computer Vision and Pattern Recognition*, pages 2656–2665, 2018.
- [23] Zhongyi Pei, Zhangjie Cao, Mingsheng Long, and Jianmin Wang. Multi-adversarial domain adaptation. In *AAAI Conference on Artificial Intelligence*, 2018.
- [24] Olga Russakovsky, Jia Deng, Hao Su, Jonathan Krause, Sanjeev Satheesh, Sean Ma, Zhiheng Huang, Andrej Karpathy, Aditya Khosla, Michael Bernstein, et al. Imagenet large scale visual recognition challenge. *International journal of computer vision*, 115(3):211–252, 2015.
- [25] Kate Saenko, Brian Kulis, Mario Fritz, and Trevor Darrell. Adapting visual category models to new domains. In *European conference on computer vision*, pages 213–226. Springer, 2010.
- [26] Kuniaki Saito, Yoshitaka Ushiku, and Tatsuya Harada. Asymmetric tri-training for unsupervised domain adaptation. In *International Conference on Machine Learning*, pages 2988–2997, 2017.
- [27] Kuniaki Saito, Kohei Watanabe, Yoshitaka Ushiku, and Tatsuya Harada. Maximum classifier discrepancy for unsupervised domain adaptation. In *The IEEE Conference on Computer Vision and Pattern Recognition (CVPR)*, June 2018.
- [28] Swami Sankaranarayanan, Yogesh Balaji, Carlos D. Castillo, and Rama Chellappa. Generate to adapt: Aligning domains using generative adversarial networks. In *The IEEE Conference on Computer Vision and Pattern Recognition (CVPR)*, June 2018.
- [29] Florian Schroff, Dmitry Kalenichenko, and James Philbin. Facenet: A unified embedding for face recognition and clustering. In *Proceedings of the IEEE conference on computer vision and pattern recognition*, pages 815–823, 2015.
- [30] Ozan Sener, Hyun Oh Song, Ashutosh Saxena, and Silvio Savarese. Learning transferrable representations for unsupervised domain adaptation. In *Advances in Neural Information Processing Systems*, pages 2110–2118, 2016.
- [31] Hidetoshi Shimodaira. Improving predictive inference under covariate shift by weighting the log-likelihood function. *Journal of statistical planning and inference*, 90(2): 227–244, 2000.

- [32] Rui Shu, Hung Bui, Hirokazu Narui, and Stefano Ermon. A DIRT-t approach to unsupervised domain adaptation. In *International Conference on Learning Representations*, 2018.
- [33] Nitish Srivastava, Geoffrey Hinton, Alex Krizhevsky, Ilya Sutskever, and Ruslan Salakhutdinov. Dropout: a simple way to prevent neural networks from overfitting. *The Journal of Machine Learning Research*, 15(1):1929–1958, 2014.
- [34] Antti Tarvainen and Harri Valpola. Mean teachers are better role models: Weight-averaged consistency targets improve semi-supervised deep learning results. In *Advances in neural information processing systems*, pages 1195–1204, 2017.
- [35] Yi-Hsuan Tsai, Wei-Chih Hung, Samuel Schulter, Kihyuk Sohn, Ming-Hsuan Yang, and Manmohan Chandraker. Learning to adapt structured output space for semantic segmentation. In *Proceedings of the IEEE Conference on Computer Vision and Pattern Recognition*, pages 7472–7481, 2018.
- [36] Eric Tzeng, Judy Hoffman, Kate Saenko, and Trevor Darrell. Adversarial discriminative domain adaptation. In *Computer Vision and Pattern Recognition (CVPR)*, volume 1, page 4, 2017.
- [37] Hemanth Venkateswara, Jose Eusebio, Shayok Chakraborty, and Sethuraman Panchanathan. Deep hashing network for unsupervised domain adaptation. In *Computer Vision and Pattern Recognition (CVPR), 2017 IEEE Conference on*, pages 5385–5394. IEEE, 2017.
- [38] Shaoan Xie, Zibin Zheng, Liang Chen, and Chuan Chen. Learning semantic representations for unsupervised domain adaptation. In *International Conference on Machine Learning*, pages 5419–5428, 2018.
- [39] Weichen Zhang, Wanli Ouyang, Wen Li, and Dong Xu. Collaborative and adversarial network for unsupervised domain adaptation. In *Proceedings of the IEEE Conference on Computer Vision and Pattern Recognition*, pages 3801–3809, 2018.